

## Absorption Edge of Impure Gallium Arsenide

J. I. PANKOVE

RCA Laboratories, Princeton, New Jersey

(Received 22 March 1965; revised manuscript received 10 June 1965)

The exponential absorption edge of GaAs may be interpreted as reflecting the presence of tails of states extending both intrinsic bands into the energy gap. The distribution of these tail states seems exponential, varying with energy as  $\exp(E/E_0)$  where  $E_0$  increases with doping.  $E_0$  starts rising rapidly with doping at lower concentrations in  $n$ -type material than in  $p$ -type GaAs. The temperature dependence of the absorption edge is larger than that of the energy gap; this can be attributed to a strongly temperature-dependent shift of the Fermi level in agreement with the model of tailing of states.

## INTRODUCTION

ALL the absorption measurements performed on gallium arsenide to date, even on the purest material, yield an absorption spectrum which, for photons of energy lower than that of the band gap, differs from theoretical expectations based on direct transitions between parabolic bands. For momentum-conserving transitions between parabolic bands, the theory<sup>1</sup> predicts a very steeply rising absorption edge:  $\alpha = A(h\nu - E_g)^{1/2}$  ( $\alpha$  is the absorption coefficient;  $A$  is a constant;  $h\nu$  is the photon energy;  $E_g$  is the energy gap). There should be no absorption for  $h\nu < E_g$ . In fact, in many cases,<sup>2-9</sup> where data are available over a large range of absorption coefficient, the absorption edge rises exponentially over several decades of  $\alpha$ , as evidenced by a straight line on a semilogarithmic plot. An exponential dependence of the absorption edge on  $h\nu$  is sometimes referred to as Urbach's rule. Urbach<sup>10</sup> found that in a number of materials  $d \ln \alpha / d h \nu = -1/kT$ . In the present work, however,  $d \ln \alpha / d h \nu$  is not strongly dependent on temperature but varies with the impurity concentration. It is the purpose of this study to explore the significance of this gradual edge and if possible to relate it to the presence of tails of states in the energy gap.

We shall first consider the manifestation of tails of states, then describe the experimental procedure, and finally discuss the results.

## TAILS OF STATES

The introduction of a high concentration of impurities in a perfect semiconducting crystal causes a perturbation of the band structure with the result that

the parabolic distribution of the states will be disturbed and prolonged by a tail extending into the energy gap.<sup>11</sup> This effect has received considerable attention in the case of germanium.<sup>12</sup> The tail of states may be due to several causes:

(1) The spatial overlap of impurity levels broadens the latter into a band.<sup>13</sup> At high concentrations, the impurity band merges with the nearest intrinsic band, Fig. 2(a). Here the tail of states is due to the smearing of the impurity levels. However, this adds a tail to only one band [for example the conduction band as shown in Fig. 2(a)]. At low temperature, this tail of final states, being occupied by electrons, would not partici-

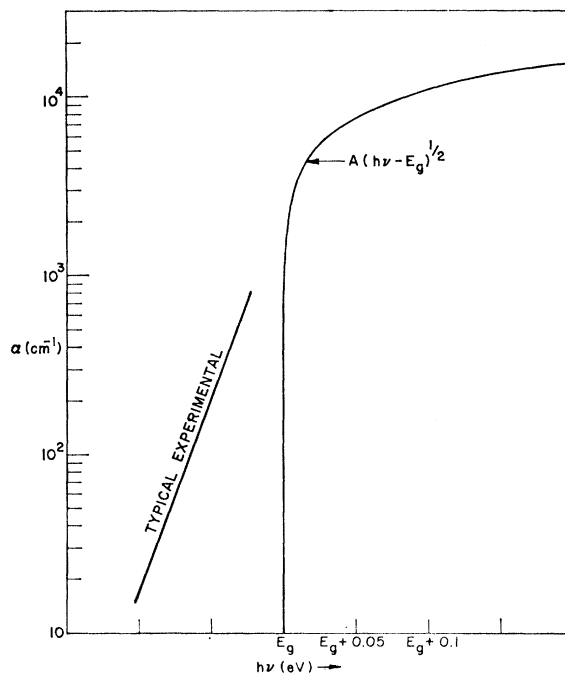


FIG. 1. Qualitative behavior of the absorption edge.

<sup>1</sup> R. A. Smith, *Semiconductors* (Cambridge University Press, New York, 1959), p. 193.

<sup>2</sup> T. S. Moss, *J. Appl. Phys.* **32**, 2136 (1961).

<sup>3</sup> M. D. Sturge, *Phys. Rev.* **127**, 768 (1962).

<sup>4</sup> W. J. Turner and W. E. Reese, *J. Applied Phys.* **35**, 350 (1964).

<sup>5</sup> D. E. Hill, *Phys. Rev.* **133**, A866 (1964).

<sup>6</sup> C. M. Chang, Stanford Electronics Laboratories Technical Report No. 5064-2 (unpublished).

<sup>7</sup> G. Lucovsky, *Appl. Phys. Letters* **5**, 37 (1964).

<sup>8</sup> I. Kudman and L. J. Vieland, *J. Phys. Chem. Solids* **24**, 967 (1963).

<sup>9</sup> W. G. Spitzer and J. M. Whelan, *Phys. Rev.* **114**, 59 (1959).

<sup>10</sup> F. Urbach, *Phys. Rev.* **92**, 1324 (1953).

<sup>11</sup> R. H. Parmenter, *Phys. Rev.* **97**, 587 (1955); V. L. Bontch-Bruевич, in *Proceedings of the International Conferences on the Physics of Semiconductors, Exeter* (The Institute of Physics and the Physical Society, London, 1962), p. 216.

<sup>12</sup> J. I. Pankove, in *Progress in Semiconductors*, edited by A. F. Gibson *et al.* (John Wiley & Sons, Inc., New York, 1965), Vol. 9.

<sup>13</sup> F. Stern and R. M. Talley, *Phys. Rev.* **100**, 1638 (1955).

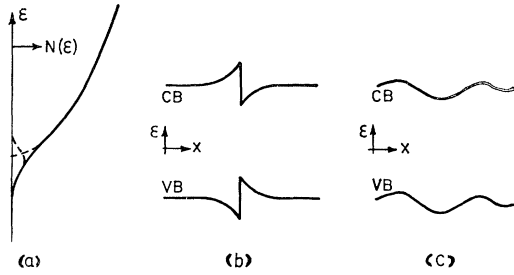


FIG. 2. Formation of tail of states by (a)–impurity banding; (b)–deformation potential; (c)–impurity-carrier interaction.

pate in the absorption process. At higher temperature, when the Fermi level is deeper in the tail, a greater change in the slope of the absorption edge would be expected. In compensated material two tails of states would be formed and both would affect the absorption.<sup>7,14</sup>

(2) The accommodation of impurities in the lattice results in localized strains (compressions and dilations). The resulting deformation potential increases locally the energy gap (compression) and elsewhere decreases it (dilation) [Fig. 2(b)].<sup>15</sup> The overall perturbation consists in smearing both band edges, making the density of states a summation of parabolas beginning at various energies. Dislocations should have the same effect.

(3) An ionized donor exerts an attractive force on the conduction electrons and a repulsive force on the valence band (acceptors act conversely). In view of the nonhomogeneous distribution of impurities (on a microscopic level), the local interaction will be more or less strong and will also smear both band edges [Fig. 2(c)].<sup>16</sup>

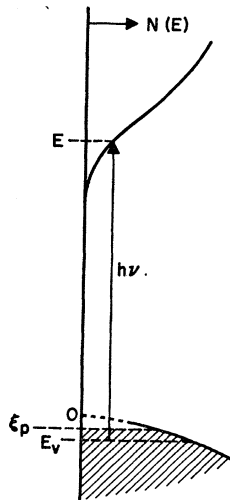


FIG. 3. Energy diagram illustrating how absorption probes the tail of states in a *p*-type semiconductor.

Let us examine how an exponential distribution of states would affect the absorption coefficient [cases (2) and (3) above]. Consider the case of a degenerate *p*-type material. The Fermi level is taken to be in the parabolic portion of the valence band, so that the perturbed part of the valence band lies above the Fermi level. Then the density of initial states,  $N_i$ , is proportional to  $(E_v)^{1/2}$ , where  $E_v$  is the energy of the state with respect to what would be the edge of the parabolic valence band (Fig. 3). The final states form an exponential tail to the conduction band and their density at some energy  $E$  is given by

$$N_f = N_0 e^{E/E_0},$$

where  $E_0$  is an empirical parameter having the dimensions of energy.  $E_0$  describes the distribution of states but not their energy assignment. Let us assume that momentum is not conserved in our optical transitions and that the matrix element for the transitions is constant, i.e., independent of the photon energy,  $h\nu = E - E_v$ . This is a reasonable assumption for heavily doped semiconductors.<sup>12</sup>

The absorption coefficient is proportional to the product of the densities of initial and final states integrated over all the possible transitions for a given  $h\nu$ :

$$\alpha(h\nu) = A \int_{\xi_p}^{h\nu - \xi_p} (E_v)^{1/2} \exp(E/E_0) dE, \quad (1)$$

where  $A$  is a constant. Let us substitute  $E - h\nu$  for  $E_0$  and make the following change of variable:

$$x = (h\nu - E)/E_0.$$

Equation (1) can be written

$$\alpha(h\nu) = -A e^{h\nu/E_0} E_0^{3/2} \int_{(h\nu + \xi_p)/E_0}^{\xi_p/E_0} x^{1/2} e^{-x} dx. \quad (2)$$

The lower limit is set to  $\infty$  because  $h\nu \gg E_0$ ; this makes the integral independent of  $h\nu$  and leads to the solution

$$\alpha(h\nu) = A E_0^{3/2} e^{h\nu/E_0} \left[ \frac{1}{2} (\pi)^{1/2} - \int_0^{\xi_p/E_0} x^{1/2} e^{-x} dx \right].$$

The slope of the absorption edge on a semilogarithmic plot then gives

$$E_0 = d h\nu / d \ln \alpha. \quad (3)$$

As mentioned in the introduction, the experimentally determined absorption edge fits an exponential dependence of  $h\nu$ . Hence, a quantity  $E_0$  can be obtained and correlated to the impurity concentration.

We have assumed in our model that doping perturbs both the conduction and the valence bands, and that the Fermi level is inside the parabolic portion of the appropriate band. The transitions will link a parabolic band with the tail of the opposite band. Hence, in

<sup>14</sup> F. Stern and J. R. Dixon, *J. Appl. Phys.* **30**, 268 (1959).  
<sup>15</sup> C. Benoit-à-la-Guille, *Ann. Phys. (Paris)* **5**, 1187 (1959).  
<sup>16</sup> V. S. Bagaiev, Yu. N. Berozashvili, B. M. Vul, E. I. Zavaritskaya, L. V. Keldysh, and A. P. Shotov, *Fiz. Tverd. Tela* **6**, 1399 (1964) [English transl.: *Soviet Phys.—Solid State* **6**, 1093 (1964)].

*n*-type material, it is the tail of the valence band which is measured, while in *p*-type material it is the conduction-band tail which affects the measurement.

**EXPERIMENTAL PROCEDURE**

The polished sample of GaAs was mounted on a copper slide provided with two identical apertures, the specimen being located over one of these apertures (Fig. 4). The copper slide was supported by a cold finger and surrounded by a thermal shield at the same temperature. The slide could be positioned magnetically to measure either the incident radiation  $I_0$  (through the unmasked aperture) or the radiation  $I$  transmitted by the sample.

The temperature of the cold finger was measured by either a carbon resistor or a GaAs thermometric diode. The carbon resistor was reliable below 50°K while the GaAs diode was sensitive above 20°K. Thus a range of overlap was available for cross checking. A test run

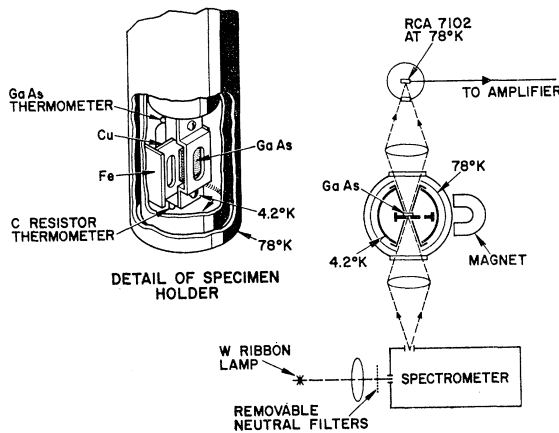


FIG. 4. Diagram of the experimental setup and detail of the specimen holder.

with a carbon resistor in lieu of a GaAs sample indicated the relative level of radiation at which the specimen might heat up. A much lower level of radiation was used. For further precaution (necessary below 4°K) the slide was set on the  $I_0$  position to completely shield the sample, except during the brief measurements.

A tungsten ribbon lamp was used as a light source. The detector consisted of an RCA 7102 photomultiplier cooled to 78°K. A double-pass Perkin-Elmer 112 spectrometer with a glass prism was used. The spectrometer was operated with a resolution of 2 meV.

The transmission of a sample of thickness  $t$  and reflectivity  $R$  is given by:

$$I = I_0 [(1-R)^2 e^{-\alpha t}] / [1 - R^2 e^{-2\alpha t}],$$

which takes into account multiple internal reflections. In our case, with  $R=0.30$  the denominator can be made 1 when  $\alpha t \geq 1.2$  (this makes an error of less than

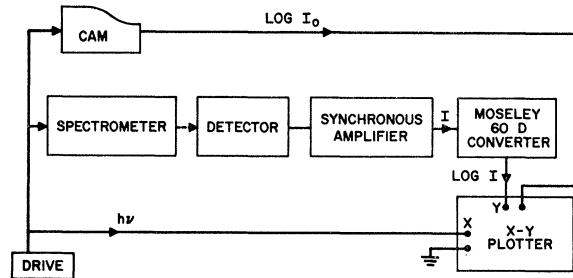


FIG. 5. Diagram of the instrumentation for plotting directly  $\alpha t$  versus  $h\nu$ .

1%); then

$$\alpha t = \ln I_0 - \ln I + 2 \ln(1-R).$$

The equipment was arranged to solve this relation directly and to plot  $\alpha t$  versus  $h\nu$ .

This was done as illustrated in Fig. 5. The logarithm of the intensity of the incident radiation  $I_0(h\nu)$  was stored on a cam driven by the spectrometer. The signal due to the transmitted radiation  $I(h\nu)$  was passed through a Moseley 60D logarithmic converter and the resulting output,  $\ln I$ , was subtracted from  $\ln I_0$  at the input of an X-Y plotter which was also driven by the spectrometer. A typical set of curves is reproduced in Fig. 6. The three calibration lines at  $\alpha t = 1.23, 3.18,$  and  $5.12$  were obtained by inserting the corresponding neutral attenuators. The ability to easily check the calibration lines made it possible to verify the system performance at any time. This was especially useful

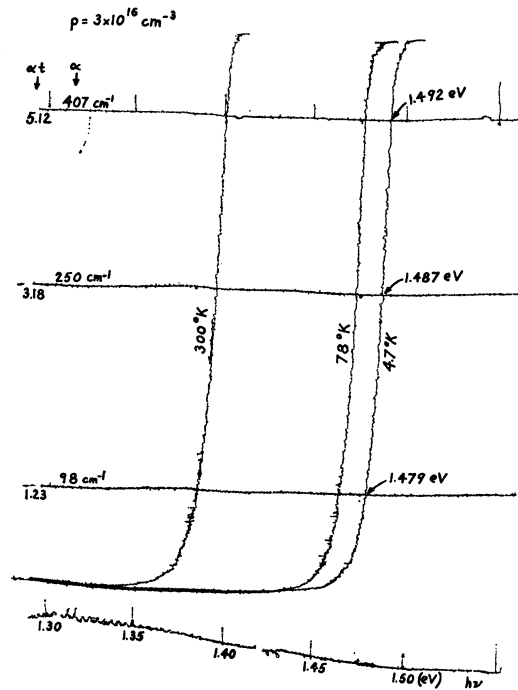


FIG. 6. A typical recording of  $\alpha t$  versus  $h\nu$ .

for detecting the cracking of a sample (the absorption curve translated to lower values of  $\alpha l$ ).

The absorption coefficient of the specimen was first recorded at room temperature, then at liquid-nitrogen temperature and then at liquid-helium temperature (actually 5°K) after waiting for equilibrium to set in. Then the He was pumped on, yielding a sample temperature of 2.1°K. When the helium was gone, the sample slowly warmed up and the temperature dependence of the absorption edge could be followed up back to room temperature. The measurement of each sample required about 6 h, the later stages of warmup being accelerated by jets of air in the cryostat chambers. Since in almost all the cases, the slope of the absorption curve did not depend on temperature, usually only the values of  $h\nu$  at  $\alpha l = 3.18$  were followed as a function of temperature.

## RESULTS

The absorption edge of a variety of *n*-type and *p*-type GaAs specimen at 5°K is shown in Fig. 7. These data were corrected for free-carrier absorption. The data for the *p*-type material with a  $1.9 \times 10^{18} \text{ cm}^{-3}$  carrier concentration were measured on two wafers having different thicknesses. Attempts at going to higher absorption coefficients by resorting to very thin wafers (a few microns thick) failed because of the excessive strains in these samples which were bonded to glass. Therefore, at the cost of a smaller range of  $\alpha$ , only samples thick enough to be self-supporting were used. One can see qualitatively that the slope of the absorption edge decreases as the carrier concentration for a given type of impurity increases. The translation of the edge along the energy axis is related to a combination of band filling (Burstein shift<sup>17</sup>) and shrinkage of the effective energy gap, as will be discussed later.

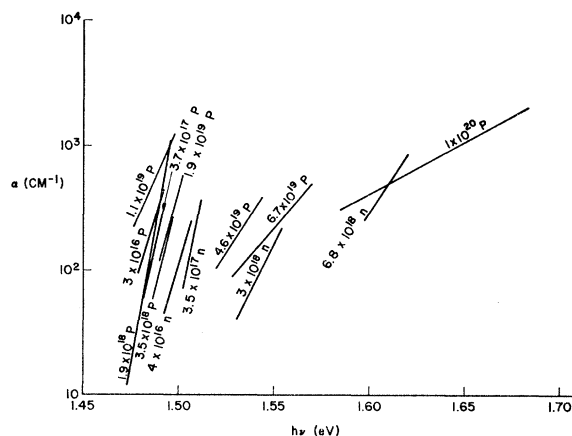


FIG. 7. Absorption edge of *n*- and *p*-type GaAs at 5°K.

<sup>17</sup> E. Burstein, Phys. Rev. **93**, 632 (1954); also T. S. Moss, Proc. Phys. Soc. (London) **B76**, 775 (1954).

A plot  $E_0$  [the reciprocal slope of the absorption edge, as per Eq. (3)] for a variety of doping is shown in Fig. 8. These data were gathered from the present measurements as well as from most of the available low-temperature published data.<sup>4-5</sup> The data of Lucovsky<sup>7</sup> on both compensated and noncompensated material show a good exponential behavior of the absorption edge between 10 and 500  $\text{cm}^{-1}$ . His  $E_0$ 's for noncompensated material agree with the rest of the data, but his  $E_0$ 's for compensated GaAs (not included in Fig. 8) are larger than could be expected from the sum of donors and acceptors. Note that in a heavily doped compensated material absorption would involve transitions between the tails of states of both valence and conduction bands. In this case the measured  $E_0$  would include the contributions of both tails. Note also that Lucovsky's data on partly compensated GaAs show

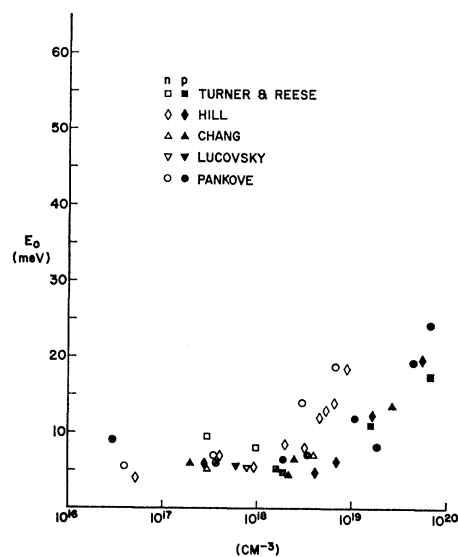


FIG. 8. Variation of the parameter  $E_0$  with carrier concentration.

that the decreased slope of the absorption edge is not due to an increase in free carriers since the carrier concentration decreases because of compensation. Not shown also are the values of  $E_0$  from Sturge's<sup>3</sup> data on semi-insulating GaAs having an ionized-impurity concentration between 3 and  $10 \times 10^{16} \text{ cm}^{-3}$ . Sturge's curves exhibit two exponential regions with  $E_0$ 's of 3 and 6 meV.

Since there is no systematic difference between the various donor impurities (Si, Se, Te) they have been represented by open symbols. There was also no systematic difference between the behaviors of acceptors (Cd and Zn). However, one can clearly see that at high concentrations tailing becomes more pronounced. Increased tailing sets in at a concentration of about  $2 \times 10^{18} \text{ cm}^{-3}$  for donors and about  $7 \times 10^{18} \text{ cm}^{-3}$  for acceptors.

We shall now consider the penetration of the Fermi level into the conduction or valence bands.

Let us arbitrarily define an "optical energy gap" for a given sample as the value of photon energy at which the absorption coefficient reaches some arbitrary level such as  $\alpha = 8000 \text{ cm}^{-1}$ . In pure GaAs, this "optical gap" is 1.515 eV at 4.2°K and 1.508 eV at 78°K, which is equal to the optical gap in pure material<sup>3</sup> corresponding to the onset of transitions between parabolic bands.

A translation of the absorption edge, at constant  $\alpha$ , to higher  $h\nu$  reflects the Burstein shift as is evident from a reconsideration<sup>18</sup> of Eq. (2). When  $\xi > E_0$ , which is true at high concentrations,  $x$  is greater than 1. Then Eq. (2) can be rewritten as

$$\alpha(h\nu) \approx A E_0^{3/2} e^{h\nu/E_0} \left( \frac{\xi_p}{E_0} \right)^{1/2} \int_{\xi_p/E_0}^{\infty} e^{-x} dx,$$

the solution of which is

$$\alpha(h\nu) \approx A E_0 \xi_p^{1/2} e^{(h\nu - \xi_p)/E_0}.$$

Therefore, for a given value of  $\alpha$ , when  $\xi_p$  and  $E_0$  increase with doping,  $h\nu$  must be increased by somewhat more than  $\xi_p$  to keep  $\alpha$  constant.

In  $n$ -type GaAs, the "optical gap" corresponds to transitions from the top of the parabolic portion of the valence band to the Fermi level in the conduction band. At low temperature, the value of  $h\nu$  at  $8000 \text{ cm}^{-1}$  measures approximately the energy gap plus the Burstein shift:  $E_g(N) + \xi(N)$ . If one subtracts from  $h\nu$  at  $8000 \text{ cm}^{-1}$ , the energy gap of pure GaAs one obtains the approximate Burstein shift reduced by any impurity-induced gap shrinkage. These data are plotted in Fig. 9. The straight line represents the penetration of the Fermi level in a purely parabolic band having an effective mass of  $0.072 m_0$ .<sup>19</sup> It is striking that, in spite of the crudity in extrapolating published data, the points follow the theoretical dependence. The fact that the experimental points are lower than the theoretical values by a nearly constant factor suggests that the gap shrinkage increases with doping. The apparent gap shrinkage is a manifestation of the tail of states in the conduction band: the Fermi level need not rise as far in the parabolic portion of the conduction band as in the unperturbed material to provide a given concentration of free carriers. Since both the theoretical and experimental values are proportional to the  $2/3$  power of the donor concentration, the gap shrinkage is also proportional to  $(N_d)^{2/3}$ . It is assumed here that the donor concentration is equal to the electron concentration. However, this assumption may be somewhat in error, at least in the case of Se, because, as was shown by Vieland and Kudman,<sup>20</sup> not all the selenium is electrically active above  $4 \times 10^{18} \text{ cm}^{-3}$ . A

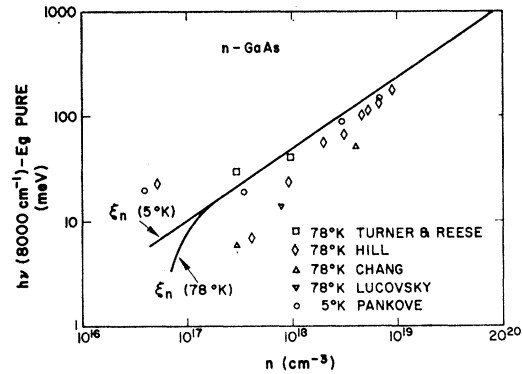


Fig. 9. Dependence of the extrapolated optical gap in  $n$ -type GaAs on electron concentration. The data are presented in such a form as to show the Burstein shift.

similar reservation can be made for high concentrations of any impurity. Another questionable assumption is the constancy of the density-of-states effective mass (the electrical-susceptibility effective mass<sup>21</sup> for the conduction band increases by 20% over the range of interest). But the theoretical curve, corrected<sup>18</sup> for the increasing effective mass, is still above the last experimental point of Fig. 9.

The data for  $p$ -type material show considerably more scatter at low concentration than the  $n$ -type material. At low acceptor concentrations one gets negative values for  $[h\nu(8000 \text{ cm}^{-1}) - E_g(\text{pure})]$ . A negative value implies that the optical gap of  $p$ -type GaAs is lower than that of pure GaAs. This shift of the absorption edge to lower energies had already been shown by measurements at room temperature.<sup>22</sup> In the case of emission, a similar shift to lower energies is attributed to the formation of an acceptor band 30 meV above the valence band.<sup>23</sup> This assumption would lead us to expect an optical absorption edge some 30 meV lower than in pure material. This is the reason for plotting  $[h\nu(8000 \text{ cm}^{-1}) - E_g(\text{pure}) + 30 \text{ meV}]$  versus carrier concentration in Fig. 10. This figure shows that the absorption edge is nearly constant up to concentrations of  $1 \times 10^{19} \text{ cm}^{-3}$ , and that the initial states are very close to the edge of the unperturbed parabolic valence band (corresponding to an ordinate of 30 meV). There is no evidence for the formation of a separate partly filled acceptor band 30 meV above the valence band nor for a substantial density of states in a tail. Above  $1 \times 10^{19} \text{ cm}^{-3}$ , the absorption edge rises more rapidly with concentration than the penetration of the Fermi level ( $\xi_p$ ) in an unperturbed parabolic valence band. The rapid rise of this absorption edge suggests that the parabolicity of the valence band is perturbed,

<sup>21</sup> M. Cardona, Phys. Rev. **121**, 752 (1961).

<sup>22</sup> D. M. Eagles, J. Phys. Chem. Solids **16**, 76 (1960). I. Kudman and T. Seidel, J. Appl. Phys. **33**, 771 (1962). R. Braunstein, J. I. Pankove, and H. Nelson, Appl. Phys. Letters **3**, 31 (1963).

<sup>23</sup> M. I. Nathan and G. Burns, Appl. Phys. Letters **1**, 98 (1962); J. I. Pankove, J. Appl. Phys. **35**, 1890 (1964).

<sup>18</sup> D. Meyerhofer (private communication).

<sup>19</sup> H. Ehrenreich, Phys. Rev. **120**, 1951 (1960).

<sup>20</sup> L. J. Vieland and I. Kudman, J. Phys. Chem. Solids **24**, 437 (1963).

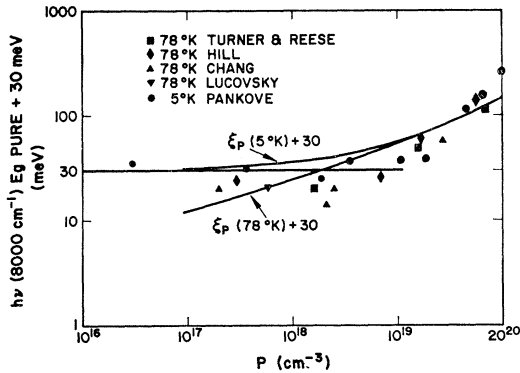


FIG. 10. Dependence of the extrapolated optical gap in *p*-type GaAs on hole concentration. The data are presented in such a way as to show the Burstein shift with respect to a 30-meV acceptor level.

perhaps by the formation of a sizable tail of states (as already suggested by Fig. 8). A perturbation of the distribution of states in the valence band causing a decrease in effective mass near the band edge would lead one to expect a greater penetration of the Fermi level into the band as the concentration increases than if the band had not been perturbed. This profound

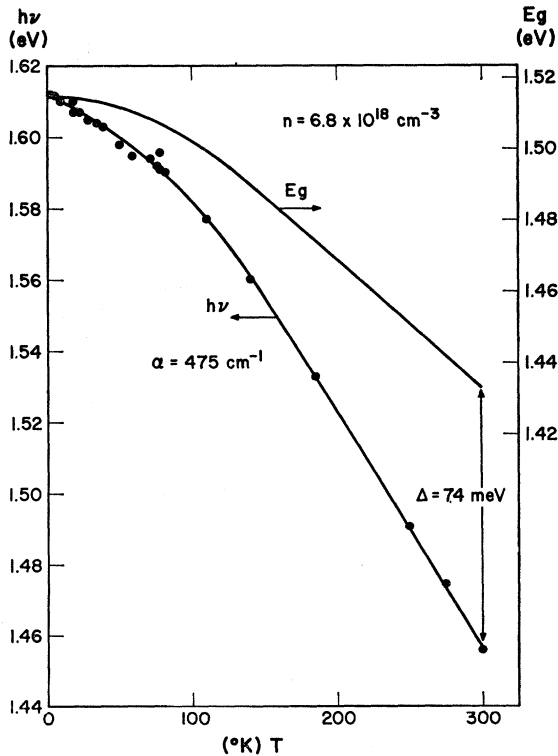


FIG. 11. Temperature dependence of the absorption edge at  $475\text{ cm}^{-1}$  (left scale) for an *n*-type sample with a carrier concentration of  $6.8 \times 10^{18}\text{ cm}^{-3}$ . For comparison, the temperature dependence of the energy gap of pure material, Eq. (3) is shown (right scale). The difference  $\Delta$  is attributed to the temperature dependence of the Fermi level.

deformation of the band structure in heavily doped *p*-type GaAs is believed to be responsible for the relatively low laser threshold current densities obtained in room-temperature injection lasers.<sup>24</sup> Our conclusion is then that for heavy doping the bands depart from a parabolic distribution of density of states near the Fermi level. Most of the carriers are in a long exponential tail.

Let us consider now the temperature dependence of the absorption edge. As stated earlier, as the temperature is varied, almost all our samples show a translation of the absorption edge without change in its slope. Figure 11 illustrates such a temperature dependence. The variation of the energy gap of pure GaAs with temperature is known.<sup>3</sup> If one compares the temperature dependent shrinkage of the absorption edge in pure and doped GaAs (as shown in Fig. 11) one finds that the shrinkage is more pronounced for the doped than for the pure material. Furthermore, the difference between these two shrinkages increases with doping.

TABLE I. Fermi-level shrinkage. (...) indicates that the calculated Fermi level is inside the energy gap.

<i>n</i>	Type	$\xi$ (2°K)	$\xi$ (300°K)	$\Delta_{\text{calc}}$	$\Delta_{\text{exp}}$
$4 \times 10^{16}$	<i>n</i>	6	...	6	24
$3.5 \times 10^{17}$	<i>n</i>	25	...	25	23
$3 \times 10^{18}$	<i>n</i>	105	99	6	64
$6.8 \times 10^{18}$	<i>n</i>	182	178	4	74
$3 \times 10^{16}$	<i>p</i>	...	...	...	18
$3.7 \times 10^{17}$	<i>p</i>	3	...	3	20
$1.9 \times 10^{18}$	<i>p</i>	8	...	8	19
$3.5 \times 10^{18}$	<i>p</i>	12	...	12	24
$1.1 \times 10^{19}$	<i>p</i>	26	...	26	30
$1.9 \times 10^{19}$	<i>p</i>	38	20	18	62
$4.6 \times 10^{19}$	<i>p</i>	70	59	11	98
$1 \times 10^{20}$	<i>p</i>	115	110	5	118

Let us define the differential shrinkage  $\Delta$  as

$$\Delta = [h\nu(2^\circ\text{K}) - h\nu(300^\circ\text{K})]_{\text{doped}} - [E_g(2^\circ\text{K}) - E_g(300^\circ\text{K})]_{\text{pure}}$$

The values of  $\Delta$  obtained from the present measurements are listed in Table I as  $\Delta_{\text{exp}}$ . Since there is no reason to believe that the temperature dependence of the energy gap is affected by doping, one must look for an additional mechanism affecting the temperature dependence of the Fermi level. As the temperature is raised, the higher energy carriers are placed in regions of higher density of states (deeper in the band), while the lower energy carriers lost by the change in the distribution function come from a region of lower density of states. Thus, to keep the carrier concentration constant, the Fermi level moves closer to the band

<sup>24</sup> G. C. Dousmanis, H. Nelson, and D. L. Stabler, *Appl. Phys. Letters* **5**, 174 (1964); H. Nelson, J. I. Pankove, F. Hawrylo, G. C. Dousmanis, and C. Reno, *Proc. IEEE* **52**, 1360 (1964); J. I. Pankove, *Proceedings of the International Symposium on Radiative Recombination, Paris, 1964* (Dunod Cie., Paris, 1965), Vol. 4, p. 201.

edge. In the case of a parabolic band, the band edge is well defined and this additional shrinkage of the absorption edge (the Fermi level shrinkage) can be calculated.<sup>25</sup> We find that it is important only when  $\xi \approx kT$ , in which case  $\Delta_{\text{calc}} \approx kT$ . The fact that our experimental  $\Delta$  are larger than  $\Delta_{\text{calc}}$  might be explained, for heavy doping, by assuming that the Fermi level is inside or near an exponential tail. Then, as the temperature increases, the Fermi-level shrinkage can be substantial.

**CONCLUSION**

The exponential absorption edge of GaAs may be interpreted as reflecting the presence of tails of states extending both intrinsic bands into the energy gap. The distribution of these tail states would be exponential, varying with energy toward the intrinsic band as  $\exp(E/E_0)$ , where  $E_0$  increases with doping.  $E_0$  starts

<sup>25</sup> J. I. Pankove and E. K. Annavedder, *J. Appl. Phys.* **36**, 3948 (1965).

rising rapidly with doping at lower concentrations in *n*-type material than in *p*-type GaAs. The density of states in the tails of *n*-type GaAs seems to grow as the  $\frac{2}{3}$  power of the electron concentrations, but the Fermi level remains in the parabolic portion of the conduction band. In *p*-type GaAs with more than  $1 \times 10^{19}$  acceptors/cm<sup>3</sup>, the valence band seems so deformed by the tail of states that near the Fermi level it no longer approximates a parabola. The temperature dependence of the absorption edge seems to follow the Fermi level into the tail, in qualitative accord with this model.

**ACKNOWLEDGMENTS**

The author is grateful to J. E. Berkeyheiser for his valuable assistance, to T. M. Stiller for help with Eq. (1) to G. C. Dousmanis, M. A. Lampert, R. H. Paramenter, and T. Seidel for enlightening discussions, and to D. Meyerhofer for his constructive review of the manuscript.

**Effect of Pressure and Magnetic Field on the Connectivity of the Fermi Surface of Zinc\***

J. E. SCHIRBER

*Sandia Laboratory, Albuquerque, New Mexico*

(Received 4 June 1965)

We report quantitative measurements of the pressure dependence (to  $\sim 6$  kbar) of the lengths of the one-dimensional angular regions of applied field producing open orbits in the basal plane in Zn ( $\delta_1$  and  $\delta_2$  whiskers). We find that both whiskers increase in length with pressure with the following slopes:  $d\delta_1/dP = 0.100 \pm 0.015$  deg/kbar,  $d\delta_2/dP = 0.07 \pm 0.01$  deg/kbar. Our results indicate that the connectivity in the basal plane is enhanced by hydrostatic pressure, as is expected from nearly-free-electron considerations. A system for obtaining  $4\pi$ -steradian magnetic field scan of a stationary sample at 4°K is described. Qualitative measurements of the effect of high magnetic field ( $\sim 60$  kOe) on the length of these whiskers showed that the length of  $\delta_2$  was not affected but that a small increase in the length of  $\delta_1$  could be detected with increasing field. The effect of pressure (to  $\sim 5$  kbar) on the period of the oscillations in the magnetoresistance associated with the minimum cross section of the needles is found to agree with the very-low-pressure He-gas work but not with work in the ice bomb or in frozen kerosene-oil mixtures. Consideration of all these results leads to a new zero-pressure assignment for the relation between Fermi-surface dimensions and the angular lengths of the whiskers. Using this assignment the following pressure derivatives of the radius  $r$  of the monster, the height  $h_N$ , of magnetic breakdown on the needles, and the height  $h_W$  of the waists of the monster are calculated:  $d \ln r/dP = -0.0009/\text{kbar}$ ,  $d \ln h_N/dP = -0.007/\text{kbar}$  and  $d \ln h_W/dP = 0.015/\text{kbar}$ . The results of our pressure measurements on Zn are consistently different from those obtained in solid pressure-transmitting media other than He. A comparison is made of the various results in the literature on the pressure dependence of the period of the oscillatory component of transport phenomena in Zn for  $H \parallel [0001]$ , which we feel demonstrates the superiority of the solid-He technique for low-temperature pressure generation in the range 0–9 kbar.

**I. INTRODUCTION**

**A**N extensive body of experimental data concerning the detailed topology of the Fermi surface of Zn has been obtained in the past several years. The nearly-free-electron model, with due consideration of spin-

orbit<sup>1,2</sup> and magnetic breakdown effects,<sup>3</sup> can account in a fairly quantitative fashion for the experimentally observed dimensions of the Fermi surface. For an anisotropic material such as Zn, the nearly-free-electron

<sup>1</sup> M. H. Cohen and L. M. Falicov, *Phys. Rev. Letters* **5**, 544 (1960).

<sup>2</sup> L. M. Falicov and M. H. Cohen, *Phys. Rev.* **130**, 92 (1963).

<sup>3</sup> M. H. Cohen and L. M. Falicov, *Phys. Rev. Letters* **7**, 231 (1961).

\* This work was supported by the U. S. Atomic Energy Commission.